HHS Public Access

Author manuscript

J Soc Cardiovasc Angiogr Interv. Author manuscript; available in PMC 2022 November 16.

Published in final edited form as:

J Soc Cardiovasc Angiogr Interv. 2022 ; 1(5): . doi:10.1016/j.jscai.2022.100400.

Fibrous Cap Thickness Predicts Stable Coronary Plaque Progression: Early Clinical Validation of a Semiautomated OCT Technology

Nicholas Kassis, MD[a,1], **Tomas Kovarnik, MD, PhD**[b], **Zhi Chen, PhD**[c], **Joseph R. Weber, MD**[a], **Brendan Martin, PhD**[a], **Amir Darki, MD**[a], **Vincent Woo, MD**[a], **Andreas Wahle, PhD**[c], **Milan Sonka, PhD**[c], **John J. Lopez, MD**[a,*]

[a]Department of Medicine, Division of Cardiology, Loyola University Medical Center, Maywood, Illinois

[b]Second Department of Medicine, Department of Cardiovascular Medicine, First Faculty of Medicine, Charles University in Prague and General University Hospital in Prague, Prague, Czech Republic

[c]Department of Electrical and Computer Engineering and Iowa Institute for Biomedical Imaging, The University of Iowa, Iowa City, Iowa

Abstract

Background: Imaging-based characteristics associated with the progression of stable coronary atherosclerotic lesions are poorly defined. Utilizing a combination of optical coherence tomography (OCT) and intravascular ultrasound (IVUS) imaging, we aimed to characterize the lesions prone to progression through clinical validation of a semiautomated OCT computational program.

Methods: Patients with stable coronary artery disease underwent nonculprit vessel imaging with IVUS and OCT at baseline and IVUS at the 12-month follow-up. After coregistration of baseline and follow-up IVUS images, paired 5-mm segments from each patient were identified, demonstrating the greatest plaque progression and regression as measured by the change in plaque burden. Experienced readers identified plaque features on corresponding baseline OCT segments, and predictors of plaque progression were assessed by multivariable analysis. Each segment then underwent volumetric assessment of the fibrous cap (FC) using proprietary software.

*Corresponding author: jlopez7@lumc.edu (J.J. Lopez).

[1]**Present address:** Department of Internal Medicine, Cleveland Clinic Foundation, Cleveland, Ohio

Declaration of competing interest

Dr Lopez is a consultant for Abbott-St Jude, runs educational training programs related to optical coherence tomography, and is an investigator in clinical trials with optical coherence tomography. Drs Kassis, Kovarnik, Chen, Weber, Martin, Darki, Woo, Wahle, and Sonka reported no financial interests.

Ethics statement

The research reported has adhered to the relevant ethical guidelines.

Supplementary material

To access the supplementary material accompanying this article, visit the online version of the *Journal of the Society for Cardiovascular Angiography & Interventions* at 10.1016/j.jscai.2022.100400.

Results: Among 23 patients (70% men; median age, 67 years), experienced-reader analysis demonstrated that for every 100 μm increase in mean FC thickness, plaques were 87% less likely to progress ($P = .01$), which persisted on multivariable analysis controlling for baseline plaque burden ($P = .05$). Automated FC analysis ($n = 17$ paired segments) confirmed this finding ($P = .01$) and found thinner minimal FC thickness ($P = .01$) and larger FC surface area of <65 μm ($P = .02$) and <100 μm ($P = .04$) in progressing segments than in regressing segments. No additional imaging features predicted plaque progression.

Conclusions: A semiautomated FC analysis tool confirmed the significant association between thinner FC and stable coronary plaque progression along entire vessel segments, illustrating the diffuse nature of FC thinning and suggesting a future clinical role in predicting the progression of stable coronary artery disease.

Keywords

coronary artery disease; intravascular ultrasound; optical coherence tomography

Introduction

Coronary arterial plaques that exhibit rapid progression are associated with a higher incidence of clinically adverse events.[1] Although several recent imaging studies have identified the characteristics of unstable coronary lesions that are associated with accelerated luminal narrowing or future coronary events, including large baseline plaque volume, large necrotic core, and thin-cap fibroatheroma (TCFA) morphology by intravascular ultrasound (IVUS) and optical coherence tomography (OCT), the features associated with the progression of stable atherosclerotic lesions are less well-characterized.[2–4] IVUS may be important in evaluating coronary disease progression by quantifying vessel size, plaque burden and distribution, and basic phenotypic plaque features through the visualization of the entire vessel wall; however, as a single modality, it is unable to resolve detailed structural plaque components such as fibrous cap (FC) thickness.[5]

Several reports have demonstrated the utility of combined intravascular imaging with IVUS and OCT to identify the role of FC thickness in atherosclerotic progression and regression,[6–9] and few reports have similarly incorporated automated software aided by expert reader guidance to analyze FC thickness.[9–12] These studies, however, primarily examined vessels during an active acute coronary syndrome. Additionally, FC measurement has traditionally been recorded at single or select time points along focal lesion segments, in turn failing to capture the 3-dimensional morphology of the true FC. In our dual-modality analysis, we sought to validate a novel, fully volumetric and comprehensive OCT computational algorithm relative to traditional experienced-reader analysis, while demonstrating whether it offers a more complete understanding of FC thickness as a potential predictor of stable coronary atherosclerotic progression.

Methods

Study patients

The Loyola University Medical Center Intravascular Imaging Database was established in 2009 and was approved by the institutional review board to allow for retrospective analysis of intravascular imaging procedures, including IVUS and OCT, performed at the time of coronary intervention. All patients within this registry of >500 subjects provided written informed consent. Included in this database are 56 patients with symptomatic stable CAD enrolled as part of the Charles University Prediction of Extent and Risk Profile of Coronary Atherosclerosis and Their Changes During Lipid-lowering Therapy Based on Non-invasive Techniques (PREDICT) trial (NCT01773512) who underwent angiography and culprit lesion percutaneous coronary intervention, with IVUS evaluation in a nonculprit vessel both at the index procedure and 12-month follow-up. We identified a subset of 31 patients from this cohort who underwent OCT imaging in the same setting as IVUS at the time of index procedure. After excluding patients with poor capture or quality of OCT images ($n = 2$) or with lack of either a progressing ($n = 5$) or regressing ($n = 1$) coronary segment within the nonculprit vessel from baseline to follow-up, 23 patients were analyzed. Of these 23 paired samples, 6 additional studies were excluded from automated FC analysis because of insufficient lipid plaque burden in either paired segment (Figure 1). Before the index procedure, baseline demographic, laboratory testing, and clinical data were recorded (Supplemental Material).

IVUS image acquisition

After coronary angiography and revascularization of the culprit lesion, IVUS gray-scale imaging of the nonculprit vessel was performed using standard techniques with an Eagle Eye 20-MHz 2.9F phased-array IVUS probe (Volcano Corporation), utilizing automatic pullback (research pullback, model R-l00) at 0.5 mm/s. Before any intravascular imaging procedure, all participants received 200 μg of intracoronary nitroglycerin to prevent catheter-induced vasospasm. IVUS was performed in an identical manner and vessel location at both baseline and follow-up time points.

OCT image acquisition

After acquiring IVUS imaging during the index procedure, OCT imaging was performed in the identical vessel segment via a frequency-domain ILUMIEN OCT catheter (St. Jude Medical). After contrast administration via power injection to create a blood-free field, OCT images were recorded at 20 mm/s for a total of 54 mm from distal to proximal within the vessel.

Target plaque identification

IVUS pullback data were stored on DVDs for offline quantitative analysis by the University of Iowa Institute for Biomedical Imaging, a highly experienced center with proprietary software analyzing IVUS/OCT imaging. Frame-by-frame coregistration of baseline and follow-up IVUS image pullbacks was performed through an optimization technique based on geometrically correct, full 3-dimensional–vessel reconstruction, a previously validated

approach with registration performance statistically identical to human experts, and plaque analysis was performed for each patient in increments of adjacent 5-mm vessel segments.[13–16] Plaque burden of each frame in both baseline and follow-up pullbacks was then calculated as follows: (external elastic membrane cross-sectional area [CSA] – lumen CSA) / external elastic membrane CSA. The absolute change in plaque burden from baseline to follow-up was defined as the difference between the averaged value of each 5-mm segment. Two 5-mm segments were identified per patient: the segment with the greatest degree of plaque progression and the segment with the greatest degree of plaque regression, as determined by the change in IVUS-derived plaque burden. With this approach, a paired sample analysis was performed. To ensure examination of identical regions between imaging modalities, IVUS images were coregistered with OCT using anatomical landmarks, including measured distances from the vessel ostium and side branches.

IVUS image analysis

All IVUS pullback frames were quantitatively analyzed for coronary plaque morphology using a proprietary in-house automated system.[13] Morphological assessment included luminal CSA, external elastic membrane CSA, eccentricity ([maximum plaque thickness – minimum plaque thickness] / maximum plaque thickness), total plaque, and plaque burden.[17] Additionally, the Liverpool Active Plaque Score, a validated method to discriminate acute coronary syndrome lesions from clinically stable lesions, was determined.[18]

OCT image analysis

Experienced readers.—OCT images were stored in DICOM format and analyzed on a dedicated offline workstation (St. Jude Medical) with LightLab Imaging software by 2 experienced readers (J.J.L., N.K.) using the previously described validated criteria.[19–21] In case of disagreement, adjudication was performed by consensus.

The minimal and mean FC thicknesses were measured at 1-mm intervals as the distance from the lumen edge to the lipid pool, with measurements obtained 3 times at the thinnest location and at randomly selected sites within the frame, respectively (Figure 2). Values for each frame were subsequently averaged. TCFA was identified as a lipid-rich plaque with an arc of ≥1 quadrant (90°) and an overlying FC below a particular threshold at its thinnest part; cap thickness cutoffs of <65 μm and <100 μm were utilized based on postmortem findings and higher thresholds used in previous studies, respectively.[22–25] Although an important component of TCFA, the presence of macrophages was not identified because of the controversial capability of OCT in delineating this feature from various plaque components such as cholesterol crystals and microcalcifications, previously demonstrating low reproducibility by expert reader analysis.[26,27] Measurements of remaining plaque features were obtained using the standard criteria (Supplemental Material).

Automated software.—Following the traditional OCT analysis by experienced readers, automated segmentation of luminal and FC surfaces was performed within each frame of the target OCT segments that contained lipid plaque, using validated software for this purpose.[28,29] This was achieved using software tracings delineated through an entirely

3-dimensional LOG-ISMOS graph-based approach developed for an intravascular OCT environment adapted to a coronary atherosclerosis scenario.[15,28] These borders were then reviewed and in the event of inaccurate border delineation, efficiently corrected by an expert reader (N.K.) using our "Just-Enough-Interaction" adjustment method, as shown in Figure 3 and described in the Supplemental Material.[13,28] The use of manual adjustment of computer-generated luminal contours is an approach that has previously been employed.[10–12] The angular range of FC in each frame was also specified by the expert reader. Using the entire extension of FC overlying lipid plaque in a segment, quantitative volumetric analyses of each 540-frame pullback were then performed to determine the mean and minimal FC thickness, percentage of frames with minimal FC thickness of <65, 100, and 200 μm, overall and percentage of total FC surface area of <65, 100, and 200 μm, mean and maximum total lipid arcs, as well as FC volume, which was calculated as FC area multiplied by frame spacing (0.1 mm in our case).[13–15,29]

Statistical analysis

All continuous measures are expressed as mean and SD or median and IQR based on their underlying distribution. Categorical risk factors are reported as frequency and proportion. Because of the presence of paired data, conditional logistic regression models were used to compare descriptive IVUS variables between segments. OCT variables were compared using exact conditional logistic regression models to estimate the odds of experiencing plaque progression as a function of univariable clinical measures. In each model, a binomial distribution was specified for the response variable, whereas logit links were used to estimate the odds ratio for each explanatory variable. A multivariable analysis of imaging features was then pursued using a 2-predictor model, owing to the limited size of the matched sample. Interobserver agreement of OCT plaque features between experienced readers was quantified using a linear mixed model to estimate the intraclass correlation coefficient in subcohorts of patients. In each comparison, random intercepts were allowed for each patient strata to account for paired cases. An alpha error rate of $P < .05$ was considered statistically significant. All analyses were performed using R 3.5.1 and SAS 9.4.

Results

A total of 31 patients met the entry criteria, and 8 patients were excluded because of poor image quality or absence of paired intravascular imaging segments. Overall, 23 subjects with stable CAD who underwent nonculprit vessel imaging with OCT and IVUS at baseline and IVUS at follow-up were included in all analyses, excluding those based on lipid plaque. An additional 6 patients did not undergo FC analysis because of insufficient lipid plaque to assess these parameters.

Patient population

As summarized in Table 1, the cohort included 70% men with a median age of 67 years. The left anterior descending artery was the nonculprit vessel most commonly (43%) imaged. All patients received a high-intensity statin as part of the PREDICT trial. All patients were taking aspirin 100 mg before vessel imaging, with nearly all subjects (96%) additionally on an angiotensin-converting enzyme inhibitor or angiotensin receptor blocker. The mean

time to follow-up from the index procedure was 12 (8, 14) months, during which 2 patients underwent percutaneous coronary intervention for stable angina (1 at the index culprit site and 1 in a new lesion). No patients underwent intervention at the nonculprit study segments of interest.

IVUS imaging features

The baseline plaque burden in both progressing (39% [33%, 59%]) and regressing (53% [45%, 58%)] segments demonstrated a moderate burden of atherosclerosis, with the baseline plaque burden ($P = .04$) and plaque area ($P = .01$) inversely related to progression (Table 2). The changes in plaque burden were modest but differed between segments (progressing +2.9 % [+1.1%, +5%] vs regressing −4.9 % [−7.5%, −1.9%], $P < .001$). Baseline Liverpool Active Plaque Score was similar between groups (progressing −0.8 vs regressing +0.3, $P =$ not significant) and well within the range of stable atherosclerotic lesions (score < 6).

OCT predictors of progression by experienced-reader analysis

Univariable and multivariable OCT analyses by experienced readers are displayed in Table 2. The presence of early atherosclerosis among segments is evidenced by the scarcity of calcified plaque (8.6% of total frames). Experienced-reader analysis demonstrated that progressing segments had significantly thinner mean FC relative to regressing segments (250 [200, 290] μm vs 260 [240, 320] μm, $P = .01$). On further analysis, plaques were 87% less likely to progress for every 100 μm increase in mean FC thickness (odds ratio, 0.13; 95% CI, 0.01–0.68; $P = .01$). After adjusting for baseline plaque burden, multivariable analysis confirmed the significant association between FC thickness and plaque progression per 100 μm increase in FC thickness (odds ratio, 0.13; 95% CI, 0.02–0.998; $P = .05$).

OCT predictors of progression by semiautomated FC analysis

As described in Table 2, a significant difference in mean FC thickness was confirmed with automated FC analysis ($P = .005$), which further demonstrated thinner minimal FC thickness ($P = .008$), higher percentage of frames with FC thickness of <65 μm ($P = .01$), larger FC surface area of <65 μm ($P = .02$), and higher percentage of total FC surface area of <65 μm ($P = .02$) in progressing segments than in regressing segments (Central Illustration).

No additional OCT features analyzed by either experienced readers or automated algorithm were predictive of segment progression, including the maximum or mean lipid arc, minimal lumen area, minimal lumen diameter, or FC volume. The identification of TCFA and plaque type did not differ between the groups (Table 2).

Reproducibility

The interobserver agreements between experienced readers in characterizing OCT image features were of good or excellent reliability and comparable to similar reported efforts.[8,30] The intraclass correlation coefficient was 0.91 for minimal FC thickness, 0.77 for mean FC thickness, 0.82 for lipid arc, and 0.90 for identification of lipid plaque.

Discussion

The morphological features of coronary plaques play a critical role in the propensity of an individual plaque to progress; therefore, an approach focused on imaging-guided identification of these features may be worth investigating. In assessing plaque progression and regression with IVUS-derived plaque burden and identifying predictive features using baseline OCT, we found that vessel segments with atherosclerotic progression had significantly thinner FC, which illustrates the importance of FC thickness as a predictor of stable plaque progression. To our knowledge, our study is among the first to employ the complementary features[24] of both modalities, OCT and IVUS, to better characterize lesion progression in stable coronary disease, and serves as an early validation of the clinical utility of a semiautomated FC measurement tool for this purpose.

Prior work largely centers on predicting unstable plaque vulnerability; however, the data on the morphological features of stable atherosclerotic progression are limited. Our investigation builds upon prior OCT reports that corroborate findings by experienced readers with a digitized, computational analysis.[10–12] This novel automated tool allowed us to volumetrically assess the true FC along entire lesion segments using more robust and detailed FC data than previously available, and in doing so, illustrate the diffuse nature of FC thinning and the significance of assessing this parameter beyond basic measures of its minimal thickness. The methodology employed in our study is in line with prior efforts[12] and may obviate the need for tedious manual image analysis by offering a more comprehensive approach to predicting plaque progression, and thereby, allowing for unique strategies to better correlate this progression with future cardiovascular events.

In evaluating patients with angiographically nonsignificant disease similar to ours, Uemura et al[31] found a greater incidence of TCFA and lipid pools among coronary plaques that developed rapid progression relative to those that failed to progress. However, this study defined progression angiographically and failed to quantify FC thickness between groups. The drawbacks of determining plaque progression and regression using coronary angiography are well-described.[32,33] Instead, IVUS is widely considered the gold standard imaging modality for measuring atheroma burden.[34,35] The use of multilayer segmentation in determining IVUS volumes in our study combined automated segmentation and subsequent computer-aided refinement, which allowed the user to produce high-quality segmentation results of clinical images. The performance of this approach is statistically indistinguishable from the independent standard for both luminal and external elastic membrane surfaces,[13–16] and it serves as the foundation on which the correctness of all derived measurements are based, including plaque burden quantification.

Further, the use of a single TCFA definition by Uemura et al[31] based on postmortem data makes it challenging to translate the findings in vivo, as a number of studies have since reported discrepancies between the pathologically determined cap threshold and in vivo critical FC thickness, presumably because of tissue shrinkage during pathological fixation and processing as well as postmortem artery contraction.[23,25,36] In our study, FC thickness was quantified in an analysis inclusive of all frames within the target segment to increase the accuracy of overall FC assessment, a feature incapable with single-frame measurement.[24]

The nonsignificant trend of TCFA of <100 μm favoring progressing relative to regressing segments and similar incidence of TCFA of <65 μm between groups, may in part be due to the absolute infrequency of TCFA in coronary arterial segments,[10] particularly in early atherosclerotic, stable disease.[20,37] Despite the thinner FC in progressing segments, the total FC volume between groups was similar, which may be explained by the greater cumulative surface area of FC in progressing segments than in regressing segments.

Prior studies have identified a relationship between plaque progression and large baseline plaque burden, yet these investigations focused on unstable, culprit plaques dissimilar to ours.[3,4] Notably, we found that progressing segments demonstrated smaller baseline plaque burden and area, a finding consistent with a recent analysis by Bourantas et al[9] that revealed that in nonculprit sites among patients admitted with a myocardial infarction, plaque regression was greater in segments with increased baseline plaque burden. With all study subjects on statin therapy, the established effects of statins on FC thickness and reducing atheroma size may help explain our findings.[8,12,34,38,39] The beneficial effects of statins are consistently greater in lesions with larger plaque burden, with the greatest degree of progression in those with the least amount of baseline plaque.[34,35,38] The findings of our multivariable analysis suggest that the impact of plaque burden on atherosclerotic evolution is at least partly dependent on FC thickness; statin therapy may have preferentially benefited regressing segments because of a larger baseline plaque burden and area and/or thicker FC.

The relationship between thinner FC and plaque progression may be due to subclinical plaque rupture and healing, mediated by repeated breaks in FC. Healed ruptures are frequent among stable plaque with mild-moderate luminal narrowing, particularly among those with healed prior myocardial infarction; 70% of our patient population experienced a prior myocardial infarction.[40,41] Nonetheless, further prospective studies are needed to elucidate the precise mechanisms of progression at the level of individual plaques, and to assess the implications of individual plaque stabilization on cardiovascular outcomes.

In determining FC thickness using OCT, Yonetsu et al[25] found that in 95% of ruptured plaques, the thinnest and most representative cap thicknesses were <80 μm and <188 μm, respectively, suggesting a higher critical threshold in vivo than that long-established by postmortem data and illustrating the diffuse nature of thinning along entire caps of lipid-rich plaques. These findings along with those of our automated analysis, which demonstrated increased FC surface area of <65 μm and <100 μm in progressing segments, challenge the use of a single FC threshold to assess for TCFA or concerning plaque progression and instead support an approach focused on complete FC analysis along entire lipid plaques. This is made possible by our automated tool, which simultaneously allows for efficient correction of segmentation errors using a 3-dimensional, regional approach in lieu of tedious and variable frame-based manual retracing.[28,29]

The main contribution of our novel tool is its inherent volumetric approach to OCT image analysis and determined quantitative indices. Although conventional manual analyses typically rely on expert-traced boundaries of coronary wall layers in a small number of OCT image frames, our method analyzes all image frames in the pullback. As a result, the measurements of wall morphology are volumetric, integrating indices that are evaluated

from a number of adjacent image frames rather than from a single measurement. Moreover, our method detects wall layer surfaces rather than individual frame-based borders, as opposed to alternative approaches that identify frame-based boundaries of wall layers separately for each frame without considering their axial context. The spatial frame-to-frame context is fully incorporated in the process of surface segmentation, avoiding frame-to-frame jumps and thus offering another level of spatial correctness.

Limitations

Several study limitations are worth noting. First, the present study included a relatively small sample size from a single center. Second, the analyzed vessels represented predominantly early-stage atherosclerosis; therefore, the findings may not apply to more advanced disease, including those with heavy calcification, as they were excluded. Finally, this was not a true natural history study because all patients received statin therapy before enrollment and throughout the study period.

Conclusions

Using combined OCT and IVUS imaging, a novel semiautomated FC measurement tool confirmed the significant association between thinner FC and stable coronary plaque progression along entire vessel segments, suggesting a future role in predicting the progression of stable atherosclerotic disease. Our findings illustrate the diffuse nature of FC thinning and the significance of assessing this parameter beyond rudimentary measures of its minimal thickness, in turn challenging the use of a single critical FC thickness threshold. The reproducibility and efficiency of our approach in measuring FC thickness offers promising applicability in large-volume studies and may ultimately obviate the practice of tedious manual OCT image analysis.

Supplementary Material

Refer to Web version on PubMed Central for supplementary material.

Acknowledgments

The authors acknowledge the entire Loyola Intravascular Imaging Research Group for supporting an exchange of ideas and for the continual expertise, as well as all personnel in the Loyola University Medical Center Cardiac Catheterization Laboratory for their assistance.

Funding sources

This work was supported by the National Institutes of Health, United States [grant numbers NIH 1T35HL120835, NIH R01 HL063373, NIH R01 EB004640]; and the Czech Health Research Council, Czechia [grant number AZV 16–28525A].

Abbreviations:

CSA	cross-sectional area
FC	fibrous cap
IVUS	intravascular ultrasound

OCT	optical coherence tomography
TCFA	thin-cap fibroatheroma

References

1. Nicholls SJ, Hsu A, Wolski K, et al. Intravascular ultrasound-derived measures of coronary atherosclerotic plaque burden and clinical outcome. J Am Coll Cardiol 2010;55(21):2399–2407. [PubMed: 20488313]
2. Stone PH, Saito S, Takahashi S, et al. Prediction of progression of coronary artery disease and clinical outcomes using vascular profiling of endothelial shear stress and arterial plaque characteristics: the PREDICTION study. Circulation 2012;126(2): 172–181. [PubMed: 22723305]
3. Stone GW, Maehara A, Lansky AJ, et al. A prospective natural-history study of coronary atherosclerosis. N Engl J Med 2011;364(3):226–235. [PubMed: 21247313]
4. Tian J, Ren X, Vergallo R, et al. Distinct morphological features of ruptured culprit plaque for acute coronary events compared to those with silent rupture and thin-cap fibroatheroma: a combined optical coherence tomography and intravascular ultrasound study. J Am Coll Cardiol 2014;63(21):2209–2216. [PubMed: 24632266]
5. Nissen SE, Yock P. Intravascular ultrasound: novel pathophysiological insights and current clinical applications. Circulation 2001;103(4):604–616. [PubMed: 11157729]
6. Diletti R, García-García HM, Gomez-Lara J, et al. Assessment of coronary atherosclerosis progression and regression at bifurcations using combined IVUS and OCT. JACC Cardiovasc Imaging 2011;4(7):774–780. [PubMed: 21757169]
7. Hou J, Xing L, Jia H, et al. Comparison of intensive versus moderate lipid-lowering therapy on fibrous cap and atheroma volume of coronary lipid-rich plaque using serial optical coherence tomography and intravascular ultrasound imaging. Am J Cardiol 2016;117(5):800–806. [PubMed: 26778524]
8. Takarada S, Imanishi T, Kubo T, et al. Effect of statin therapy on coronary fibrous-cap thickness in patients with acute coronary syndrome: assessment by optical coherence tomography study. Atherosclerosis 2009;202(2):491–497. [PubMed: 18572175]
9. Bourantas CV, Räber L, Sakellarios A, et al. Utility of multimodality intravascular imaging and the local hemodynamic forces to predict atherosclerotic disease progression. JACC Cardiovasc Imaging 2020;13(4):1021–1032. [PubMed: 31202749]
10. Raber L, Koskinas KC, Yamaji K, et al. Changes in coronary plaque composition in patients with acute myocardial infarction treated with high-intensity statin therapy (IBIS-4): a serial optical coherence tomography study. JACC Cardiovasc Imaging 2019;12(8 Pt 1):1518–1528. [PubMed: 30553686]
11. Radu MD, Yamaji K, García-García HM, et al. Variability in the measurement of minimum fibrous cap thickness and reproducibility of fibroatheroma classification by optical coherence tomography using manual versus semi-automatic assessment. EuroIntervention 2016;12(8):e987–e997. [PubMed: 27721214]
12. Nakajima A, Minami Y, Araki M, et al. Optical coherence tomography predictors for a favorable vascular response to statin therapy. J Am Heart Assoc 2021;10(1): e018205. [PubMed: 33342228]
13. Sun S, Sonka M, Beichel RR. Graph-based IVUS segmentation with efficient computer-aided refinement. IEEE Trans Med Imaging 2013;32(8):1536–1549. [PubMed: 23649180]
14. Yin Y, Zhang X, Williams R, Wu X, Anderson DD, Sonka M. LOGISMOS—layered optimal graph image segmentation of multiple objects and surfaces: cartilage segmentation in the knee joint. IEEE Trans Med Imaging 2010;29(12):2023–2037. [PubMed: 20643602]
15. Zhang L, Wahle A, Chen Z, et al. Simultaneous registration of location and orientation in intravascular ultrasound pullbacks pairs via 3D graph-based optimization. IEEE Trans Med Imaging 2015;34(12):2550–2561. [PubMed: 26080381]
16. Wahle A, Prause PM, DeJong SC, Sonka M. Geometrically correct 3-D reconstruction of intravascular ultrasound images by fusion with biplane angiography—methods and validation. IEEE Trans Med Imaging 1999;18(8):686–699. [PubMed: 10534051]

17. Mintz GS, Nissen SE, Anderson WD, et al. American College of Cardiology clinical expert consensus document on standards for acquisition, measurement and reporting of intravascular ultrasound studies (IVUS). A report of the American College of Cardiology task force on clinical expert consensus documents. J Am Coll Cardiol 2001;37(5):1478–1492. [PubMed: 11300468]
18. Murray SW, Stables RH, García-García HM, et al. Construction and validation of a plaque discrimination score from the anatomical and histological differences in coronary atherosclerosis: the Liverpool IVUS-V-HEART (Intra Vascular UltraSound-Virtual-Histology Evaluation of Atherosclerosis Requiring Treatment) study. EuroIntervention 2014;10(7):815–823. [PubMed: 24472736]
19. Tearney GJ, Regar E, Akasaka T, et al. Consensus standards for acquisition, measurement, and reporting of intravascular optical coherence tomography studies: a report from the international working group for intravascular optical coherence tomography standardization and validation. J Am Coll Cardiol 2012;59(12): 1058–1072. [PubMed: 22421299]
20. Jang IK, Tearney GJ, MacNeill B, et al. In vivo characterization of coronary atherosclerotic plaque by use of optical coherence tomography. Circulation 2005; 111(12):1551–1555. [PubMed: 15781733]
21. Yabushita H, Bouma BE, Houser SL, et al. Characterization of human atherosclerosis by optical coherence tomography. Circulation 2002;106(13):1640–1645. [PubMed: 12270856]
22. Barlis P, Serruys PW, Gonzalo N, van der Giessen WJ, de Jaegere PJ, Regar E. Assessment of culprit and remote coronary narrowings using optical coherence tomography with long-term outcomes. Am J Cardiol 2008;102(4):391–395. [PubMed: 18678293]
23. Schaar JA, de Korte CL, Mastik F, et al. Characterizing vulnerable plaque features with intravascular elastography. Circulation 2003;108(21):2636–2641. [PubMed: 14581406]
24. Brown AJ, Obaid DR, Costopoulos C, et al. Direct comparison of virtual-histology intravascular ultrasound and optical coherence tomography imaging for identification of thin-cap fibroatheroma. Circ Cardiovasc Imaging 2015;8(10): e003487. [PubMed: 26429760]
25. Yonetsu T, Kakuta T, Lee T, et al. In vivo critical fibrous cap thickness for ruptureprone coronary plaques assessed by optical coherence tomography. Eur Heart J 2011;32(10):1251–1259. [PubMed: 21273202]
26. Tearney GJ. OCT imaging of macrophages: a bright spot in the study of inflammation in human atherosclerosis. JACC Cardiovasc Imaging 2015;8(1):73–75. [PubMed: 25592697]
27. van Soest G, Regar E, Goderie TPM, et al. Pitfalls in plaque characterization by OCT: image artifacts in native coronary arteries. JACC Cardiovasc Imaging 2011;4(7): 810–813. [PubMed: 21757174]
28. Chen Z, Pazdernik M, Zhang H, et al. Quantitative 3D analysis of coronary wall morphology in heart transplant patients: OCT-assessed cardiac allograft vasculopathy progression. Med Image Anal 2018;50:95–105. [PubMed: 30253306]
29. Pazdernik M, Chen Z, Bedanova H, et al. Early detection of cardiac allograft vasculopathy using highly automated 3-dimensional optical coherence tomography analysis. J Heart Lung Transplant 2018;37(8):992–1000. [PubMed: 29706574]
30. Kato K, Yonetsu T, Kim SJ, et al. Comparison of nonculprit coronary plaque characteristics between patients with and without diabetes: a 3-vessel optical coherence tomography study. JACC Cardiovasc Interv 2012;5(11): 1150–1158. [PubMed: 23174639]
31. Uemura S, Ishigami KI, Soeda T, et al. Thin-cap fibroatheroma and microchannel findings in optical coherence tomography correlate with subsequent progression of coronary atheromatous plaques. Eur Heart J 2012;33(1):78–85. [PubMed: 21831910]
32. Ito K, Yamagishi M, Yasumura Y, Nakatani S, Yasuda S, Miyatake K. Impact of coronary artery remodeling on misinterpretation of angiographic disease eccentricity: evidence from intravascular ultrasound. Int J Cardiol 1999;70(3): 275–282. [PubMed: 10501342]
33. Isner JM, Kishel J, Kent KM, Ronan JA, Ross AM, Roberts WC. Accuracy of angiographic determination of left main coronary arterial narrowing. Angiographic–histologic correlative analysis in 28 patients. Circulation 1981; 63(5):1056–1064. [PubMed: 7471365]

34. Nissen SE, Tuzcu EM, Schoenhagen P, et al. Effect of intensive compared with moderate lipid-lowering therapy on progression of coronary atherosclerosis: a randomized controlled trial. JAMA 2004;291(9):1071–1080. [PubMed: 14996776]

35. Nissen SE, Tsunoda T, Tuzcu EM, et al. Effect of recombinant ApoA-I Milano on coronary atherosclerosis in patients with acute coronary syndromes: a randomized controlled trial. JAMA 2003;290(17):2292–2300. [PubMed: 14600188]

36. Fishbein MC, Siegel RJ. How big are coronary atherosclerotic plaques that rupture? Circulation 1996;94(10):2662–2666. [PubMed: 8921814]

37. Cheruvu PK, Finn AV, Gardner C, et al. Frequency and distribution of thin-cap fibroatheroma and ruptured plaques in human coronary arteries: a pathologic study. J Am Coll Cardiol 2007;50(10):940–949. [PubMed: 17765120]

38. Hattori K, Ozaki Y, Ismail TF, et al. Impact of statin therapy on plaque characteristics as assessed by serial OCT, grayscale and integrated backscatter-IVUS. JACC Cardiovasc Imaging 2012;5(2):169–177. [PubMed: 22340823]

39. Nissen SE, Nicholls SJ, Sipahi I, et al. Effect of very high-intensity statin therapy on regression of coronary atherosclerosis: the ASTEROID trial. JAMA 2006;295(13): 1556–1565. [PubMed: 16533939]

40. Burke AP, Kolodgie FD, Farb A, et al. Healed plaque ruptures and sudden coronary death: evidence that subclinical rupture has a role in plaque progression. Circulation 2001;103(7):934–940. [PubMed: 11181466]

41. Vergallo R, Porto I, D'Amario D, et al. Coronary atherosclerotic phenotype and plaque healing in patients with recurrent acute coronary syndromes compared with patients with long-term clinical stability: an in vivo optical coherence tomography study. JAMA Cardiol 2019;4(4):321–329. [PubMed: 30865212]

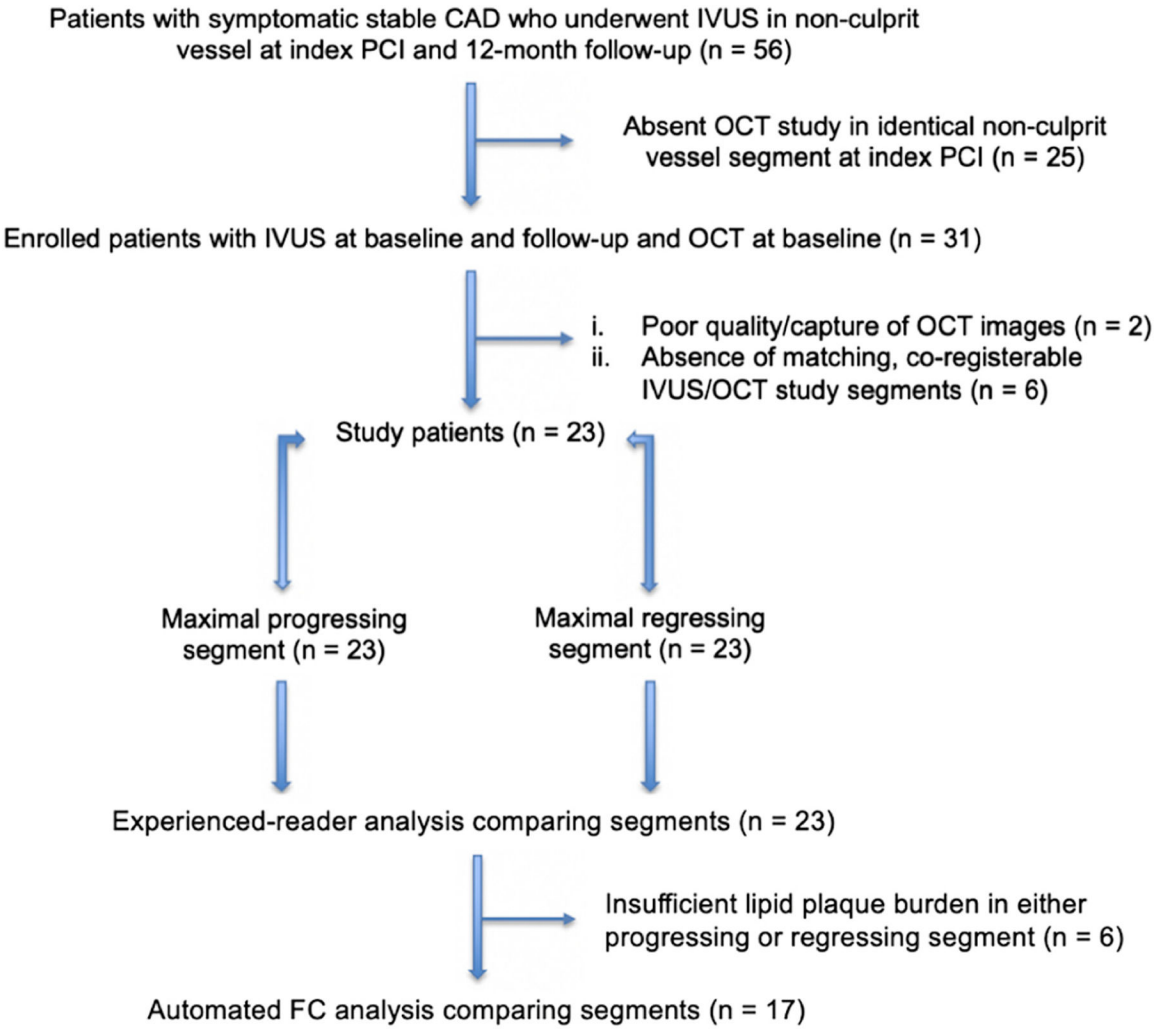

Figure. 1. Flowchart of study patient selection.

A total of 23 subjects with stable coronary artery disease who underwent nonculprit vessel imaging with optical coherence tomography and intravascular ultrasound at baseline and intrvascular ultrasound at follow-up were included in the study. Of these, 6 patients did not undergo fibrous cap analysis due to insufficient lipid plaque to assess these parameters. CAD, coronary artery disease; FC, fibrous cap; IVUS, intravascular ultrasound; OCT, optical coherence tomography; PCI, percutaneous coronary intervention.

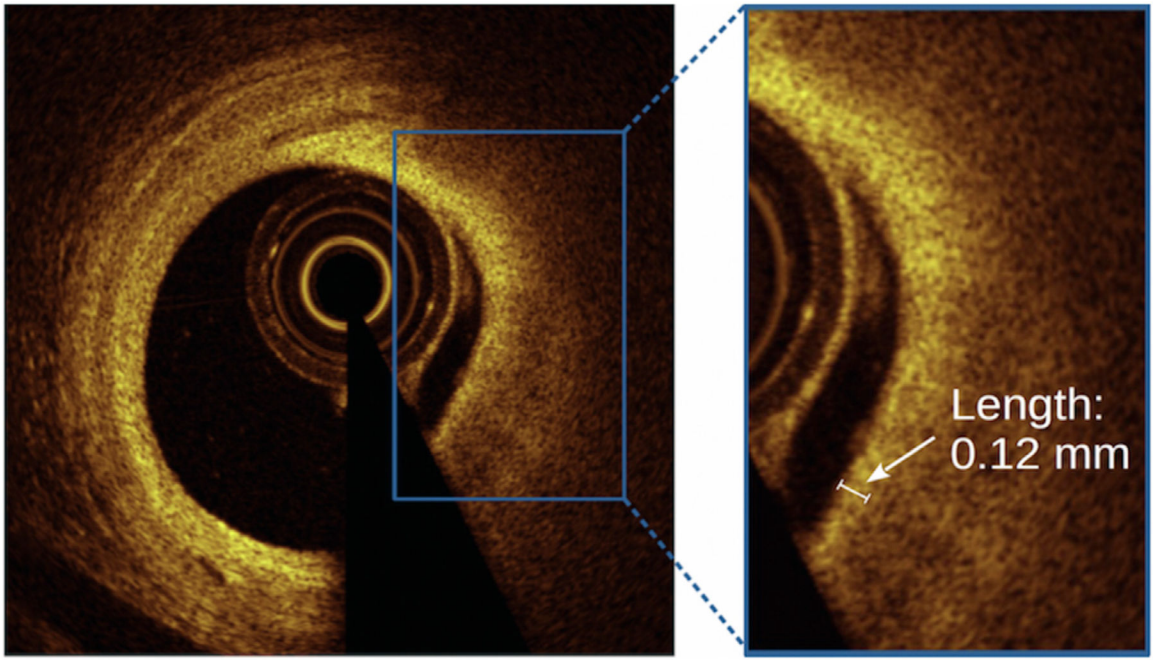

Figure. 2. Reader measurement of fibrous cap thickness.

Cross-sectional OCT images of signal-rich fibrous cap overlying a signal-poor lipid pool. The inset demonstrates the measurement of fibrous cap thickness (white arrow) within a frame, achieved using a length measurement tool on an offline OCT workstation. OCT, optical coherence tomography.

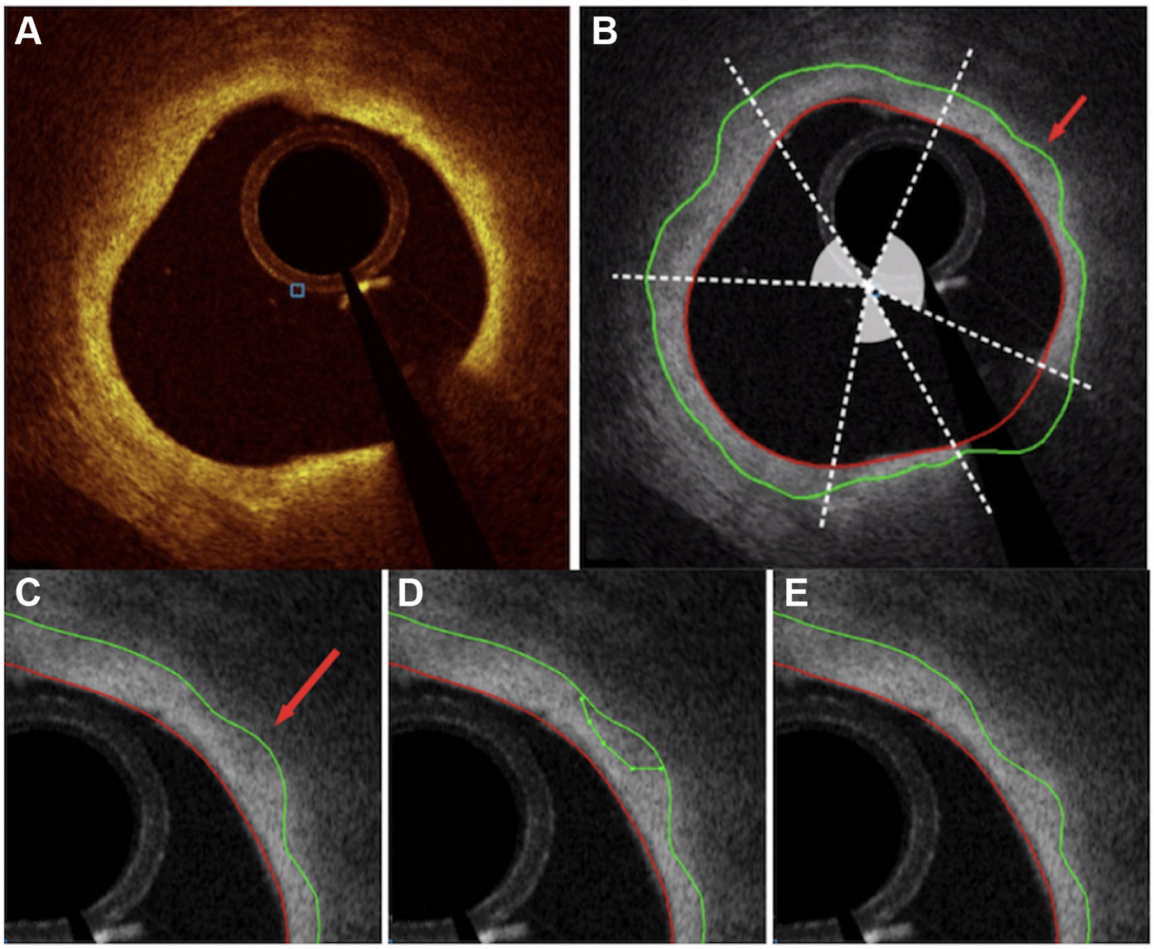

Figure. 3. JEI tool enabling manual correction of automatic wall layer analysis.

(**A**) Original cross-sectional optical coherence tomography image of the lipid-rich plaque. (**B**) Angular range of FC overlying the lipid-rich plaque, denoted by shaded arcs. (**C**) Automated segmentation of FC (green line) and lumen (red line) using multilayer approach, demonstrating an inaccuracy (red arrow) in border delineation. (**D**) FC border correction by experienced reader using the JEI adjustment method. (**E**) Optimized, recomputed 3-dimensional–connected surfaces after JEI. FC, fibrous cap; JEI, Just-Enough-Interaction.

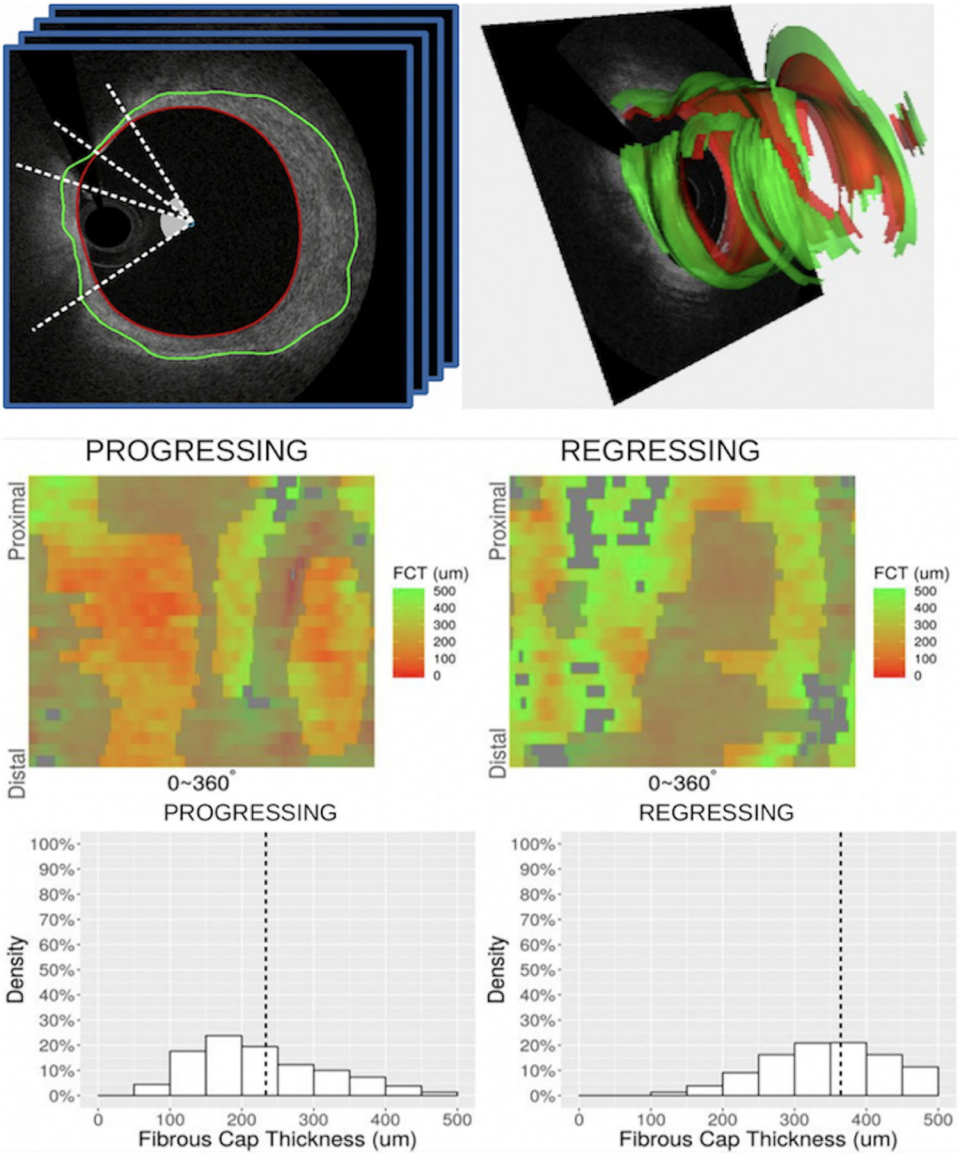

Central Illustration. Carpet map characterization of FC thickness in progressing vs regressing segment of a single representative patient.

The top panel illustrates the extraction of cap thicknesses from our automated FC assessment tool. The middle panel demonstrates color-coded gradations of FCT displayed longitudinally (y-axis) and circumferentially (x-axis) on an unwrapped vessel wall. The shadowed areas represent nonmeasurable regions caused by guidewire shadow, residual blood, and exclusion regions without lipid pool. The bottom panel highlights the clustering of these cap thicknesses between groups, with the vertical dot line indicating the average FCT for each group. FC, fibrous cap; FCT, fibrous cap thickness.

Table 1.

Patient characteristics.

	***N* = 23**
Age, y	66.8 ± 9.5
Male	16 (70)
Female	7 (30)
Body mass index, kg/m^2	27.9 ± 4.3
Follow-up, mos (range)	12 (8–14)
CAD risk factors	
Prior tobacco use	12 (52)
Current tobacco use	5 (22)
Diabetes mellitus	5 (22)
Hypertension	22 (96)
Hyperlipidemia	20 (87)
Previous myocardial infarction	16 (70)
Family history of CAD	11 (48)
Medications at index procedure	
Aspirin	23 (100)
Calcium channel blocker	10 (43)
Statin	23 (100)
ACE-I/ARB	22 (96)
Beta-blocker	17 (74)
Baseline laboratory data	
LDL, mg/dL	83 ± 32
HDL, mg/dL	49 ± 16
Total cholesterol, mg/dL	155 ± 36
Triglycerides, mg/dL	128 ± 53
Lipoprotein(a), mg/dL	34 ± 32
hs-CRP, mg/L	1.3 ± 1.5
MMP-9, ng/mL	3.7 ± 3.7
12-Month laboratory data	
LDL, mg/dL	56 ± 15
HDL, mg/dL	46 ± 10
Total cholesterol, mg/dL	125 ± 21
Triglycerides, mg/dL	114 ± 43
Lipoprotein(a), mg/dL	38 ± 42
hs-CRP, mg/L	2.4 ± 4.3
MMP-9, ng/mL	5.2 ± 4.3
Imaged vessel	
Left anterior descending artery	10 (43)
Left circumflex artery	6 (26)
Right coronary artery	7 (30)

Data are presented as mean ± SD for continuous variables and *n* (%) for categorical variables. Missing laboratory data were omitted from calculations.

ACE-I/ARB, angiotensin-converting enzyme inhibitor/angiotensin receptor blocker; CAD, coronary artery disease; HDL, high-density lipoprotein; hs-CRP, high sensitivity C-reactive protein; LDL, low-density lipoprotein; MMP-9, matrix metalloproteinase-9.

Table 2.

Intravascular imaging features of stable coronary plaque progression.

Variable	Progressing (*n* = 23)	Regressing (*n* = 23)	Odds ratio (95% CI)	*P* value
Intravascular ultrasound				
Baseline				
Plaque burden, %	39 (33, 59)	53 (45, 58)	-	.04
Plaque area, mm^2	6.5 (4.8, 9.7)	9 (7.3, 10.9)	-	.01
Eccentricity	0.8 (0.73, 0.87)	0.78 (0.57, 0.86)	-	ns
EEM size, mm^2	15.8 (13.3, 18.7)	16.2 (13.1, 22)	-	ns
LAPS	−0.8 (−1.4, 0.5)	0.3 (−0.96, 2)	-	ns
Follow-up				
Plaque burden, %	45 (38, 58)	47 (39, 54)	-	ns
Plaque area, mm^2	7.2 (5.3, 9.3)	7.5 (6.4, 8.4)	-	ns
Eccentricity	0.81 (0.62, 0.87)	0.77 (0.64, 0.88)	-	ns
EEM size, mm^2	16.6 (12.8, 18.9)	15.2 (12.8, 21.4)	-	ns
LAPS	−0.61 (−1.5, 0.5)	−0.28 (−1.3, 0.83)	-	ns
Δ Baseline follow-up				
Plaque burden, %	2.9 (1.1, 5)	−4.9 (−7.5, −1.9)	-	<.001
Plaque area, mm^2	0.53 (0.17, 1.3)	−1.1 (−1.7, −0.5)	-	<.001
Eccentricity	0.004 (−0.01, 0.03)	0.02 (−0.02, 0.07)	-	ns
EEM size, mm^2	0.12 (−0.15, 0.89)	−0.52 (−0.85, 0.08)	-	.003
LAPS	−0.02 (−0.43, 0.33)	−0.23 (−1.5, 0.33)	-	.05
Plaque area, mm^2			-	<.001
Eccentricity			-	ns
EEM size, mm^2			-	.003
LAPS			-	.05
Optical coherence tomography[a]				
Quantitative index				
MLA, mm^2	4.5 (4, 6.4)	5 (3.8, 7)	0.9 (0.7–1.2)	ns

J Soc Cardiovasc Angiogr Interv. Author manuscript; available in PMC 2022 November 16.

Variable	Progressing (*n* = 23)	Regressing (*n* = 23)	Odds ratio (95% CI)	*P* value
MLD, mm	2.3 (1.9, 2.7)	2.1 (2, 2.7)	0.8 (0.3–2.5)	ns
% area stenosis	37 (20, 54)	37 (14, 48)	2.4 (0.2–37.2)	ns
Mean lipid arc, °	102 (35, 194)	101 (0, 163)	1 (1–1)	ns
Maximum lipid arc, °	150 (97, 290)	140 (0, 219)	1 (1–1)	ns
Mean calcium arc, °	0 (0, 8)	9 (0, 39)	1 (1–1)	ns
Maximum calcium arc, °	0 (0, 38)	40 (0, 84)	1 (1–1)	ns
Reference lumen area, mm^2	7.9 (6.8, 9.6)	7.5 (4.9, 11.4)	1 (0.9–1.2)	ns
Reference mean diameter, mm	3.2 (2.9, 3.5)	3.1 (2.5, 3.8)	1.2 (0.5–3.4)	ns
Minimal FCT, µm[b]	90 (80, 150)	100 (70, 130)	0.3 (0.02–3.5)	ns
Mean FCT, µm[b]	250 (200, 290)	260 (240, 320)	0.1 (0.01–0.7)	.01
TCFA <65 µm	3 (13)	3 (13)	1.8 (0.4–13.3)	ns
TCFA <100 µm	12 (51)	8 (34)	1.4 (0.8–3.3)	ns
Plaque type (*N* = 575 frames)				
Lipid	334 (58)	315 (55)	1 (0.9–1.3)	ns
Calcified	48 (8)	51 (9)	1 (1–1)	ns
Fibrocalcific	83 (14)	69 (12)	1 (1–1.1)	ns
No plaque	110 (19)	140 (24)	1 (1–1)	ns
Multivariable logistic regression of predictive imaging features[c]				
Baseline plaque burden, %	-	-	0.71 (0.36–1.4)	.32
Average FCT, µm[b]	-	-	0.13 (0.02–0.998)	.05
Semiautomated volumetric FC analysis (*N* = 17 pairs)[d]				
Mean FCT, µm	243 ± 57	294 ± 79	-	.005
Minimal FCT, µm	56 ± 50	96 ± 73	-	.008
Frames with FCT <65 µm, %	13 ± 18	6 ± 12	-	.01
Frames with FCT <100 µm, %	36 ± 28	20 ± 27	-	<.001
Frames with FCT <200 µm, %	82 ± 24	65 ± 34	-	.04
Total FC SA <65 µm, mm^2	0.03 ± 0.05	0.01 ± 0.02	-	.02
Total FC SA <100 µm, mm^2	0.3 ± 0.4	0.2 ± 0.3	-	.04

J Soc Cardiovasc Angiogr Interv. Author manuscript; available in PMC 2022 November 16.

Variable	Progressing (*n* = 23)	Regressing (*n* = 23)	Odds ratio (95% CI)	*P* value
Total FC SA <200 μm, mm^2	4.9 ± 4.7	3.2 ± 4.4	-	ns
Total FC SA <65 μm, %	0.2 ± 0.3	0.2 ± 0.6	-	.02
Total FC SA <100 μm, %	2 ± 3	1 ± 3	-	.03
Total FC SA <200 μm, %	28 ± 21	17 ± 22	-	ns
FC volume, mm^3	3.8 ± 2.4	4.6 ± 3.8	-	ns
Mean lipid arc	134 ± 63	135 ± 87	-	ns
Maximum lipid arc	197 ± 81	184 ± 94	-	ns

Data are presented as median (25th, 75th percentile) for continuous variables, *n* (%) for categorical variables, and mean ± SD for features by automated FC analysis. Lipid arcs, FCT, and TCFA, as well as calcium arcs were only calculated in patients with identifiable lipid or calcium plaques, respectively. Of 23 paired samples, 17 pairs had analyzable lipid plaque. TCFA denotes the number of segments with at least 1 TCFA of <65 μm or <100 μm.

EEM, external elastic membrane; FC, fibrous cap; FCT, fibrous cap thickness; LAPS, Liverpool Active Plaque Score; MLA, minimal lumen area; MLD, minimal lumen diameter; ns, nonsignificant; SA, surface area; TCFA, thin-cap fibroatheroma.

[a]Experienced-reader analysis. Exact conditional logistic regression models were used to estimate the odds of experiencing plaque progression as a function of univariable clinical measures.

[b]Odds ratio per 100 μm increase in FCT.

[c]Multivariable analysis using the 2-predictor model because of the limited size of the matched sample.

[d]Optical coherence tomography-based segment-level analysis.